Published August 6, 2012, doi:10.4049/jimmunol.1201399

Role of Mincle in Alveolar Macrophage-Dependent Innate Immunity against Mycobacterial Infections in Mice

Friederike Behler,* Kathrin Steinwede,* Luciana Balboa,† Bianca Ueberberg,* Regina Maus,* Gabriele Kirchhof,* Sho Yamasaki,‡ Tobias Welte,§ and Ulrich A. Maus*

The role of macrophage-inducible C-type lectin Mincle in lung innate immunity against mycobacterial infection is incompletely defined. In this study, we show that wild-type (WT) mice responded with a delayed Mincle induction on resident alveolar macrophages and newly immigrating exudate macrophages to infection with *Mycobacterium bovis* bacillus Calmette-Guérin (BCG), peaking by days 14–21 posttreatment. As compared with WT mice, Mincle knockout (KO) mice exhibited decreased proinflammatory mediator responses and leukocyte recruitment upon *M. bovis* BCG challenge, and they demonstrated increased mycobacterial loads in pulmonary and extrapulmonary organ systems. Secondary mycobacterial infection on day 14 after primary BCG challenge led to increased cytokine gene expression in sorted alveolar macrophages of WT mice, but not Mincle KO mice, resulting in substantially reduced alveolar neutrophil recruitment and increased mycobacterial loads in the lungs of Mincle KO mice. Collectively, these data show that WT mice respond with a relatively late Mincle expression on lung sentinel cells to *M. bovis* BCG infection. Moreover, *M. bovis* BCG-induced upregulation of C-type lectin Mincle on professional phagocytes critically shapes antimycobacterial responses in both pulmonary and extrapulmonary organ systems of mice, which may be important for elucidating the role of Mincle in the control of mycobacterial dissemination in mice. *The Journal of Immunology*, **2012, 189: 000–000.**

Tuberculosis (TB) is the second leading cause of death from infectious disease worldwide. *Mycobacterium tuberculosis* is the causative pathogen of TB and remains a major global health threat. In 2010, ~8.8 million new TB cases and ~1.4 million deaths owing to TB have been reported (1). The development of multidrug-resistant *M. tuberculosis* strains has significantly complicated and limited therapeutic interventions of TB treatments, particularly in developing countries. The only approved currently available vaccine, *Mycobacterium bovis* bacillus Calmette-Guérin (BCG), has proven to be of limited efficacy against adult TB (2). Therefore, it is of vital importance to gain a better understanding of the dynamic host/pathogen interplay in TB to identify novel therapeutic targets.

M. tuberculosis is transmitted via aerosol droplets into the lungs, where alveolar macrophages (AM) constitute the primary target cell for inhaled mycobacteria (3). AM acting as lung sentinel cells protect the lungs against both apathogenic and pathogenic particles, and as such are equipped with various pattern recognition receptors, including TLRs and C-type lectin receptors. They are capable of sensing mycobacterial pathogen-associated molecular patterns (PAMPs) and of initiating innate and adaptive immune responses against invading mycobacterial pathogens. Innate immunity against lung mycobacterial infections is particularly shaped by the release of proinflammatory Th1 cytokines such as TNF-α, IL-12, and IFN-γ, which orchestrate both recruitment and activation of inflammatory leukocytes as part of the subsequently developing lung granulomas (4, 5).

The macrophage-inducible C-type lectin Mincle (also called Clec4e or Clecsf9) was originally identified as a downstream target of NF-IL-6 (C/EBPβ) in murine peritoneal macrophages, and it was found to be strongly induced in murine peritoneal macrophages in response to several inflammatory stimuli, including LPS, TNF-α, IL-6, IFN-γ, and cellular stresses (6). Similarly, in rats Mincle was found to be expressed by myeloid cells, including dendritic cells, macrophages, and neutrophils, but also by B and T cells, but not by NK cells (7). Mincle is an activating receptor interacting with the ITAM-containing adaptor molecule FcRγ (8). Mincle has been shown to serve as a receptor for SAP130, a component of small nuclear ribonucleoprotein released from dead cells (8). More recently, Mincle has been identified as a receptor for the mycobacterial cell wall component trehalose-6′,6-dimycolate (TDM, cord factor) of *M. tuberculosis*, which plays a role in granuloma formation, as well as its synthetic analog trehalose-6′,6-dibehenate (4, 9, 10). Moreover, Mincle is also an activating receptor for the pathogenic fungi *Candida albicans* and *Malassezia* (11, 12).

Ligation of Mincle initiates a downstream signaling leading to activation of the kinase Syk that is linked to triggering a protein complex of CARD9 with the adaptor BCL10 and paracaspase MALT1, resulting in canonical activation of NF-κB (13), with downstream induction of innate immune and inflammatory responses following microbial infection and tissue damage (13). A more recent study suggested a role for neutrophils in promoting TDM-induced lung inflammation via the Mincle pathway (14). However, there are only very limited in vivo data available addressing the role of Mincle as AM activator and regulator of antimycobacterial

*Department of Experimental Pneumology, Hannover Medical School, Hannover 30625, Germany; †Instituto de Medicina Experimental, Consejo Nacional de Investigaciones Científicas y Técnicas de Argentina, Academia Nacional de Medicina, 1425 Buenos Aires, Argentina; ‡Division of Molecular Immunology, Medical Institute of Bioregulation, Kyushu University, Fukuoka 812-8582, Japan; and §Clinic for Pneumology, Hannover Medical School, Hannover 30625, Germany

Received for publication May 16, 2012. Accepted for publication July 13, 2012.

This work was supported by a grant from the German Research Foundation (to U.A.M.).

Address correspondence and reprint requests to Prof. Ulrich A. Maus, Department of Experimental Pneumology, Hannover Medical School, Feodor-Lynen-Strasse 21, Hannover 30625, Germany. E-mail address: Maus.Ulrich@mh-hannover.de

Abbreviations used in this article: AM, alveolar macrophage; BAL, bronchoalveolar lavage; BCG, bacillus Calmette-Guérin; dLN, draining lymph node; FSC-A, forward scatter area; HSA, human serum albumin; KO, knockout; LAM, lipoarabinomannan; LP, lipoprotein; MOI, multiplicity of infection; PAMP, pathogen-associated molecular pattern; PIM, phosphatidylinositol mannoside; SSC-A, side scatter area; TB, tuberculosis; TDM, trehalose-6′,6-dimycolate; WT, wild-type.

responses in mice (14). Therefore, in the present study, we examined the expression profile of Mincle on resident AM as well as inflammatory elicited lung exudate macrophages and neutrophils and its role in protective immunity against *M. bovis* BCG challenge in mice.

Materials and Methods

Reagents

Purified lipoarabinomannan (LAM), phosphatidylinositol mannoside (PIM), and 19-kDa lipoprotein (LP) were purchased from the Mycobacteria Research Laboratories at Colorado State University. TDM and PKH26-GL were purchased from Sigma-Aldrich (Steinheim, Germany). FCS and accutase were purchased from PAA (Coelbe, Germany). Abs used in the present study for flow cytometry analysis were anti-CD11c PE-Cy5.5 (clone N418), anti-CD11b PE-Cy7 (clone M1/70), anti-MHC class II PE (clone M5/114.15.2), anti–Gr-1 PE (clone RB6-8C5), biotinylated mouse anti-rat IgG1 (clone RG 11/39.4), rat anti-mouse IgG1 (clone R3-34), and allophycocyanin-streptavidin. All Abs were purchased from BD Biosciences (Heidelberg, Germany). Anti-F4/80 FITC (clone Cl:A3-1) was obtained from Serotec (Düsseldorf, Germany). Monoclonal anti-Mincle Ab (clone 1B6, IgG1) was generated as recently described (8). Rat IgG control Abs were purchased from Sigma-Aldrich.

Mice

Wild-type (WT) C57BL/6J mice were purchased from Charles River Laboratories. Mincle-deficient mice on a C57BL/6J background were generated as previously described (12) and were obtained from the Consortium for Functional Glycomics. Mice were used for experiments at the age of 8–12 wk. All animal experiments were carried out in accordance with the guidelines of the Animal Care and Use Committee of the Central Animal Facility of Hannover Medical School and were approved by local government authorities.

Culture and labeling of M. bovis *BCG with PKH26*

M. bovis BCG (strain Pasteur) was cultured in Middelbrook 7H9 medium (BD Biosciences) until midlog phase and then frozen in 1-ml aliquots at −80°C

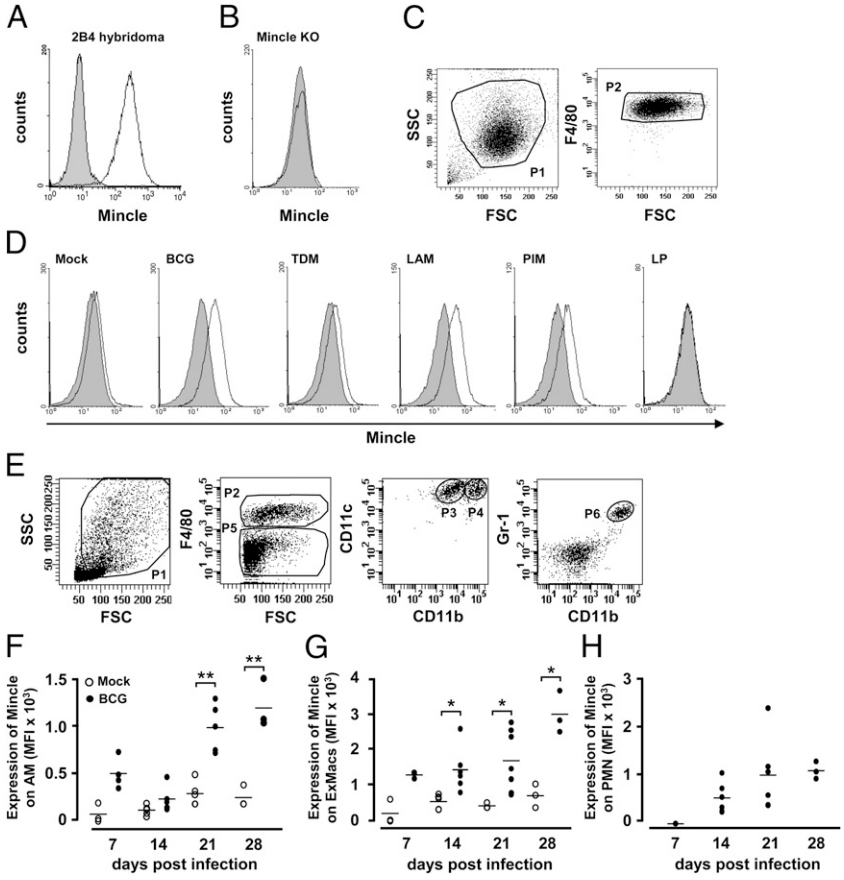

FIGURE 1. Analysis of Mincle expression on AM in vitro and in mice challenged with *M. bovis* BCG. (**A**) Mincle-expressing 2B4 T cell hybridoma cells were employed as positive Ab staining control. The gray histogram represents isotype Ab staining of 2B4 T cell hybridoma cells, and the histogram overlay (solid black line) represents 2B4 hybridoma cells stained with biotinylated anti-Mincle Ab, followed by staining of the cells with streptavidin-PE. (**B**) AM collected from untreated Mincle KO mice were infected with *M. bovis* BCG (MOI of 1) for 24 h and were then stained with isotype control (gray histogram) or anti-Mincle Ab (solid line overlay) to exclude unspecific binding of anti-Mincle Ab to BCG-infected AM. (**C**) FACS gating strategy for identification of AM of WT mice. (**D**) Pooled AM collected from five untreated WT mice were distributed at a density of 2×10^5 cells per well to 24-well culture plates and were either stimulated with vehicle (Mock) or were stimulated for 24 h with 1 μg/ml TDM, LAM, PIM, LP, or *M. bovis* BCG (MOI of 1). Subsequently, AM were harvested and gated according to their FSC-A versus SSC-A (P1) followed by hierarchical subgating according to their FSC-A versus F4/80 cell surface expression (P2), as shown in (C), followed by analysis of their Mincle cell surface expression by flow cytometry, as indicated. The shown FACS profiles are representative of three independently performed experiments with similar results. (**E**) Gating strategy for analysis of Mincle expression on professional phagocyte subsets in BCG-infected WT mice. WT mice were either mock-infected (PBS/0.1% HSA) (white dots in (F) and (G)) or were infected intratracheally with *M. bovis* BCG (3×10^5 CFU/mouse) [black dots in (**F**)–(**H**)]). BAL fluid cells were gated according to their FSC-A versus SSC-A characteristics (P1), followed by hierarchical subgating of autofluorescent lung macrophages (P2), which were composed of resident AM (P3), and autofluorescent exudate macrophages (P4). Neutrophils were gated according to their FSC/SSC profile (P1) and were characterized as low autofluorescent (P5) and $CD11b^{high}Gr\text{-}1^{high}$ cells (P6). At days 7, 14, 21, and 28, BCG-infected WT mice were subjected to BAL and expression of Mincle was analyzed on the cell surface of AM (F), exudate macrophages (G), and neutrophils (H), as indicated. Values are shown as dot plots with median values indicated as horizontal bars (n = 3–4 mock-infected mice and n = 5–7 BCG-infected mice were analyzed per time point, except for day 28, where n = 3 mice were analyzed. *$p < 0.05$, ** $p < 0.01$, relative to mock-infected mice.

until use, as previously described (15, 16). For quantification of CFU, mycobacteria were serially diluted in Middlebrook 7H9 medium and plated on 7H10 Middlebrook agar plates (BD Biosciences) followed by CFU determination after 3 wk incubation at 37°C.

To specifically analyze changes in proinflammatory gene expression profiles of BCG-phagocytosing WT as compared with Mincle-deficient AM in mice, *M. bovis* BCG was labeled with the lipophilic red fluorescent dye PKH26-GL prior to intratracheal instillation into the lungs of mice (15). PKH staining of *M. bovis* BCG in vitro resulted in a strong red fluorescence emission of mycobacteria, which was subsequently exploited for intra-alveolar tracking and subsequent sorting of mycobacteria-phagocytosing AM of PKH-BCG–infected WT and Mincle KO mice, as described previously (15). Briefly, aliquots of *M. bovis* BCG were washed in PBS (PAA) and resuspended in 1 ml diluent C (Sigma-Aldrich), followed by fluorescent staining of *M. bovis* BCG with PKH26-GL in a final concentration of 30 μM for 1 h at room temperature. Termination of the labeling process was achieved by addition of FCS. Subsequently, mycobacteria were washed twice in PBS, and the pellet was resuspended in PBS supplemented with 0.1% human serum albumin (HSA) (Behring, Hattersheim, Germany). Successful PKH labeling of BCG was verified by determination of their red fluorescence emission profile on a BD FACSCanto flow cytometer.

Infection of mice with M. bovis *BCG*

WT mice and Mincle KO mice were anesthetized by i.m. application of tetrazoline hydrochloride (2.5 mg/kg, Rompun; Bayer, Leverkusen, Germany) and ketamine (50 mg/kg; Albrecht, Aulendorf, Germany) and were subsequently infected intratracheally with a low dose of 2–3 $\times$ 10^5 CFU *M. bovis* BCG per mouse (17). In selected experiments, mice of either experimental group were infected with BCG at 8 $\times$ 10^5 CFU per mouse via lateral tail vein injection, according to previous reports (15). After instillation, mice were kept in individually ventilated cages with free access to autoclaved food and water. In selected experiments, WT mice and Mincle KO mice were infected with PKH26-stained *M. bovis* BCG at day 0, followed by reinfection of the mice with *M. bovis* BCG on day 14. Subsequently, mice were subjected to bronchoalveolar lavage (BAL) for high-speed cell sorting of PKH26-BCG–phagocytosing AM at 6 and 48 h after the second BCG infection. Sorted AM were then subjected to real-time RT-PCR analysis of proinflammatory gene expression profiles, as outlined below, using flow-sorted AM of untreated WT mice and untreated Mincle KO mice as controls.

BAL and isolation of lungs, spleen, and lung draining lymph nodes for determination of mycobacterial loads

BAL was performed as described previously (15, 18, 19). Briefly, mice were euthanized with an overdose of isoflurane (Baxter, Unterschleissheim, Germany) and BAL was performed by repeated intratracheal instillation of 300-μl aliquots of cold PBS supplemented with ETDA into the lungs of mice, followed by careful aspiration until an initial BAL fluid volume of 1.5 ml was collected. BAL was then continued until an additional BAL fluid volume of 4.5 ml was collected. Total BAL fluid cells in the 1.5- and 4.5-ml aliquots were counted and leukocyte differentials in BAL fluids were determined on Pappenheim-stained cytospin preparations. The remaining BAL cells were lysed in 0.1% saponin in HBSS (pH 7.2) (PAA) for 10 min at 37°C and then plated at 10-fold serial dilutions on 7H10 Middlebrook agar plates. Isolated lung lobes, lung draining lymph nodes (dLN), and spleens of WT and Mincle KO mice were homogenized with a tissue homogenizer (IKA, Staufen, Germany). The resulting lung and spleen homogenates were lysed in HBSS containing 0.1% saponin and 10-fold serial dilutions of homogenates were processed for determination of CFU on 7H10 agar plates. CFU in lung dLN were determined by incubation of lung dLN in 0.1% saponin (pH 7.2) for 10 min at 37°C, as well as additional incubation of dLN in an ultrasonic bath for 10 min. Subsequently, lung dLN were crushed using a pistil and homogenates were plated at 10-fold serial dilutions on 7H10 agar plates for 3 wk at 37°C (15, 17, 19).

Immunophenotypic analysis of resident and alveolar recruited mononuclear phagocyte subsets in BAL fluids of WT and Mincle KO mice

Mock-infected and *M. bovis* BCG-infected WT mice and Mincle KO mice were subjected to BAL, as described above. Identification and quantification of resident AM and alveolar recruited exudate macrophages contained in BAL fluids of mice of the respective experimental groups was done based on immunophenotypic analysis of differential cell surface Ag expression profiles. Briefly, 2 $\times$ 10^5 BAL fluid cells were incubated with Octagam (Octapharma, Langenfeld, Germany) to block Fc receptors and were then incubated with carefully titrated fluorochrome-labeled mAbs with specificity for CD11b, CD11c, MHC class II, and F4/80. Subsequently, cells were washed and subjected to FACS analysis of their cell surface Ag expression profiles. AM were gated according to their forward scatter area (FSC-A) versus side scatter area (SSC-A) characteristics, followed by hierarchical subgating according to their FSC-A versus F4/80-FITC cell surface Ag expression. According to this gating strategy, resident AM were characterized according to their green autofluorescence in conjunction with their F4/80$^+$CD11b$^-$CD11c$^+$MHC class II$^{-/low}$ Ag expression profile, and green autofluorescent alveolar exudate macrophages were characterized by their F4/80$^+$CD11b$^+$CD11c$^+$MHC class II$^{-/low}$ Ag expression profile. Subsequently, appropriately gated resident AM and exudate macrophages were analyzed for their Mincle cell surface expression. Identification of BAL fluid neutrophils and lymphocytes was done on Pappenheim-stained cytospin preparations, based on overall morphologic characteristics, including

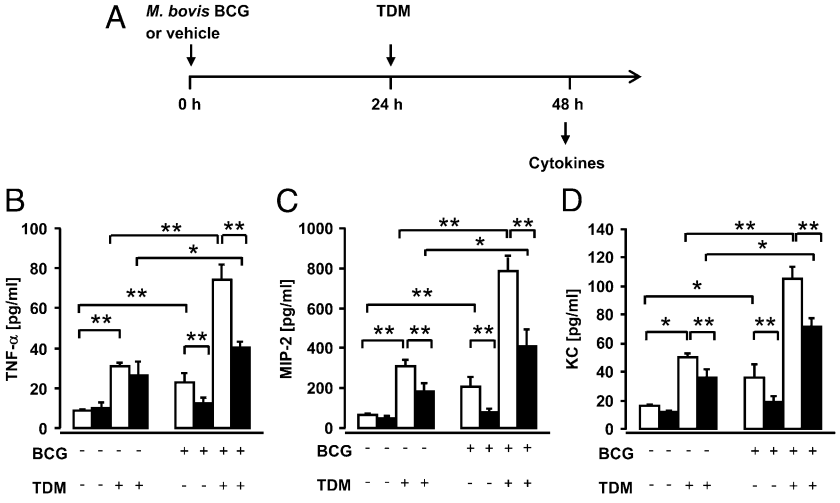

FIGURE 2. Effect of Mincle on cytokine release by *M. bovis* BCG-infected primary AM subsequently challenged with TDM. (**A**) Experimental profile. AM were collected from five WT mice (open bars) and five Mincle KO mice (filled bars). Pooled AM from WT versus Mincle KO mice were then seeded into 24-well ultra-low cluster plates at 2 $\times$ 10^5 AM/well. Cells were either 1) vehicle-treated, 2) vehicle-treated for 24 h and then stimulated with TDM for 24 h, 3) infected with *M. bovis* BCG (MOI of 1) for 24 h and then vehicle treated for 24 h, or 4) infected with *M. bovis* BCG for 24 h, followed by stimulation with TDM for 24 h, as indicated (for experimental details, see *Materials and Methods*). Subsequently, cell-free cell culture supernatants were collected and analyzed for TNF-α (**B**), MIP-2 (**C**), and KC (**D**) cytokine levels by ELISA (n = 6 determinations per experimental condition, except for vehicle-treated only cells, where n = 4 determinations). Values are shown as means ± SD. The experiment is representative of three independently performed experiments. *$p < 0.05$, ** $p < 0.01$, as indicated.

differences in cell size and nuclear shape as well as cytoplasmic staining patterns (17, 18).

Stimulation of AM with mycobacterial PAMPs for analysis of Mincle expression in vitro

AM were isolated from untreated WT mice and were plated at 2×10^5 cells per well (>99% purity) in RPMI 1640 plus 10% FCS (both PAA). Cells were either mock-infected or were infected with *M. bovis* BCG (multiplicity of infection [MOI] of 1), or they were stimulated with LAM, PIM, 19-kDa LP, or TDM (1 μg/ml final concentration). For TDM stimulation experiments, 24-well cell culture plates were prepared by coating the wells with TDM dissolved at 1 μg/ml in isopropanol, followed by incubation at room temperature under a laminar flow hood until the solvent was completely evaporated. Subsequently, cells were added to the wells as described above, and 24 h later, AM were harvested and subjected to analysis of Mincle cell surface expression on a BD FACSCanto flow cytometer. Briefly, cells were pretreated with Octagam, followed by staining of cells with either anti-Mincle Ab (clone 1B6) or isotype IgG1 Ab (clone R3-34; BD Biosciences) for 20 min on ice. After washing, cells were stained with a secondary biotinylated mouse-anti-rat IgG1 (clone RG11/39.4; BD Biosciences) for another 20 min on ice. Subsequently, cells were washed twice and incubated with streptavidin-allophycocyanin for 5 min, after which cells were washed and analyzed on a BD FACSCanto flow cytometer. The same staining protocol was employed for analysis of Mincle expression on the cell surface of mock-infected or BCG-infected WT mice (see above). As a positive control, Mincle-expressing 2B4 T cell hybridoma cells were either stained with biotinylated isotype control or biotinylated anti-Mincle Ab on ice. After washing, cells were incubated with PE-labeled streptavidin for 5 min and were then analyzed on a BD FACSCanto flow cytometer. In selected experiments, AM collected from Mincle KO mice were stained with anti-Mincle Ab, as described for staining of WT AM, to control for unspecific Ab binding to the cell surface of AM.

Stimulation of AM of WT mice and Mincle KO mice with M. bovis *BCG and/or TDM in vitro*

In selected experiments, we determined the effect of a previous *M. bovis* BCG infection of AM from WT or Mincle KO mice on their TDM-induced proinflammatory cytokine release in vitro. Briefly, WT mice and Mincle KO mice were subjected to BAL and collected WT and Mincle KO AM were then pooled and seeded into 24-well ultra-low cluster plates (Costar, Corning) in RPMI 1640/10% FCS at densities of 2×10^5 cells per well. Cells were either 1) vehicle-treated; 2) vehicle-treated for 24 h, followed by stimulation with TDM for 24 h; 3) infected with *M. bovis* BCG (MOI of 1) for 24 h, followed by vehicle treatment for 24 h; or 4) infected with *M. bovis* BCG for 24 h, followed by stimulation with TDM for another 24 h. Subsequently, cell culture supernatants were subjected to analysis of proinflammatory cytokine levels by ELISA. Coating of the wells with TDM was done essentially as described above.

Flow sorting of M. bovis *BCG-phagocytosing AM*

A high-speed FACSAria II flow cytometer (BD Biosciences) equipped with a blue laser operating at 488 nm excitation wavelength and an aerosol management system was used for sorting of *M. bovis* BCG-phagocytosing AM. Briefly, cells from BAL fluids of either mock-infected or BCG-infected WT and Mincle KO mice were collected and spun at 1400 rpm for 10 min at 4°C. Cell pellets were immediately resuspended in RPMI 1640 medium and subsequently filtered through sterile 40-μm cell strainers to remove cell aggregates. A BD FACSAria II high-speed cell sorter was prepared for aseptic sorting according to the manufacturer's instructions. AM were gated according to their FSC-A versus SSC-A characteristics as well as FSC-A versus green autofluorescence characteristics (FL1-A, FITC channel). Subsequently, those AM exhibiting an increased red fluorescence emission profile owing to phagocytosis of PKH26-labeled *M. bovis* BCG were gated according to their green autofluorescence versus increased red PKH26 fluorescence emission profile (15). After appropriate gating and compensation settings, cells were sorted at a constant flow rate of ~10,000 particles per second, using an 85-μm nozzle and sample agitation turned on. The complete sorting process (presorting of BAL fluid samples and postsorting of *M. bovis* BCG-phagocytosing AM) was performed at a constant temperature of 4°C and was finished with a resort analysis of sorted cells to verify sort purities, which were always >95% (15).

Real-time RT-PCR

Total cellular RNA was isolated from flow-sorted AM of mock-infected or *M. bovis* BCG-phagocytosing AM of WT and Mincle KO mice collected at 6 and 48 h after secondary infection with *M. bovis* BCG, or it was isolated from sorted AM of untreated control mice, using the RNeasy Micro kit (Qiagen, Hilden, Germany), following the manufacturer's instructions. Total cellular RNA quantification was determined using a NanoDrop 1000 UV-Vis spectrophotometer, and 100 ng total RNA was used for subsequent cDNA synthesis. Real-time RT-PCR assays were performed using an ABI 7500 real-time PCR system, according to the manufacturer's instructions, using SYBR Green dye (Eurogentec, San Diego, CA) (18, 19). For normalization, β-actin was used as the housekeeping gene and mean fold changes were calculated using the $2^{-\Delta\Delta Ct}$ method (20). The employed primers (Table I) for real-time PCR analysis of proinflammatory cytokine genes were designed using Primer Express software v2.0 following primer design guidelines as recommended by the manucfacturer (Applied Biosystems, Warrington, U.K.).

ELISA

Analysis of BAL fluid proinflammatory cytokines (TNF-α, CCL2, KC, MIP-2, RANTES, and IFN-γ) in culture supernatants of stimulated primary AM or BAL fluids of mock-infected or *M. bovis* BCG-infected WT and Mincle KO mice was performed using commercially available ELISAs, according to the manufacturer's instructions (R&D Systems, Wiesbaden, Germany). Detection limits of the employed ELISA assays were: TNF-α, 2 pg/ml; CCL2, 2 pg/ml; KC, 2 pg/ml; MIP-2, 1.5 pg/ml; RANTES, 2 pg/ml; IFN-γ, 2 pg/ml. In those cases where cytokine levels from undiluted BAL fluids exceeded upper detection limits of the respective ELISA, samples were diluted 1:10

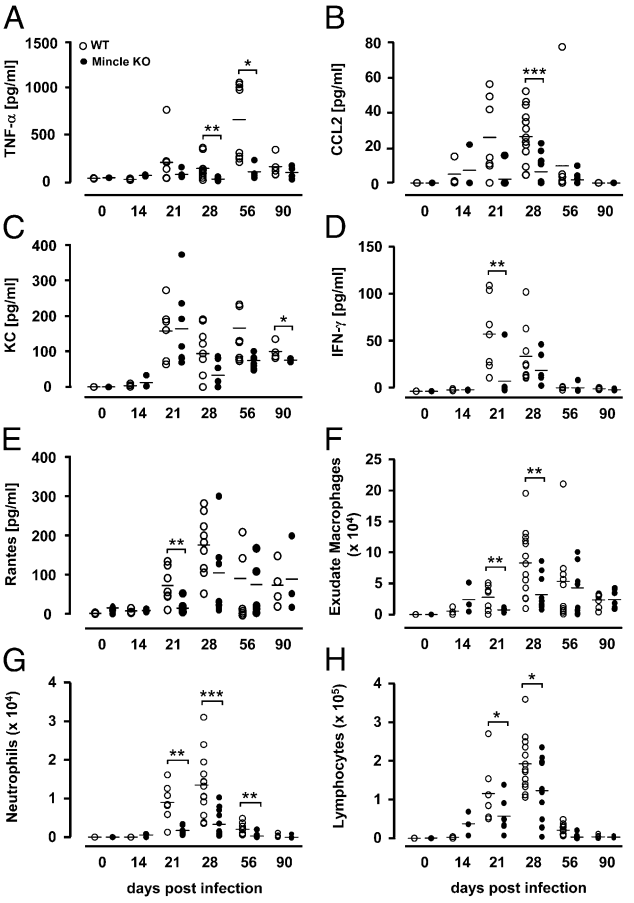

FIGURE 3. Effect of Mincle on proinflammatory cytokine release and alveolar leukocyte recruitment in *M. bovis* BCG-infected WT and Mincle KO mice. WT mice and Mincle KO mice were infected intratracheally with *M. bovis* BCG (2–3 × 10^5 CFU/mouse). At indicated time points, mice were subjected to BAL for determination of BAL fluid cytokines TNF-α (**A**), CCL2 (**B**), KC (**C**), IFN-γ (**D**), and RANTES (**E**), as well as quantification of exudate macrophages (**F**), neutrophils (**G**), and lymphocytes (**H**) in BAL fluids, as indicated. Data are shown for $n = 3$ mice (0 h time point), or 5–13 mice per time point and treatment group, except for day 90, where $n = 4$ mice per treatment group. Horizontal bar, median value. $^*p < 0.05$, $^{**}p < 0.01$, $^{***}p < 0.001$, relative to WT mice.

with PBS while taking dilution factors for calculation of final cytokine levels into account.

Statistical analysis

Data are either given as means ± SD or as dot plots with horizontal lines representing median values of the respective data sets. Data were analyzed by a nonparametric Mann–Whitney *U* test using an SPSS for Windows software package. Statistically significant differences between various treatment groups were assumed when p values were <0.05.

Results

Mincle is induced on AM in response to mycobacterial PAMPs in vitro and in response to M. bovis *BCG in mice*

In initial experiments, we assessed the specificity of the employed anti-Mincle Ab 1B6. As shown in Fig. 1A, anti-Mincle Ab 1B6 exhibited a strong binding to Mincle-expressing 2B4 T cell hybridoma cells used as a positive control. In contrast, anti-Mincle Ab did not bind to BCG-infected AM (24 h, MOI 1) collected from Mincle KO mice (Fig. 1B).

We next examined the effect of different mycobacterial PAMPs such as TDM, LAM, PIM, or 19-kDa LP from *M. tuberculosis* as well as live *M. bovis* BCG to upregulate expression of Mincle on AM in vitro and in vivo. The employed gating strategy for identification of AM from WT and Mincle KO mice is shown in Fig. 1C. Baseline expression of Mincle by mock-infected AM of WT mice was very low but detectable (Fig. 1D). Mincle expression was upregulated on AM postinfection with *M. bovis* BCG, but also after stimulation with TDM, or the mycobacterial glycolipids PIM and LAM, but not mycobacterial 19-kDa LP, within 24 h posttreatment (Fig. 1D). These data indicate that defined α1,2-mannose–containing mycobacterial molecules as well as intact BCG but not mycobacterial lipopeptides can stimulate primary AM to increased Mincle expression in vitro.

We next examined the kinetics of Mincle expression profiles on resident AM (P3, Fig. 1E) and inflammatory elicited lung exudate macrophages (P4, Fig. 1E) and alveolar neutrophils (P6, Fig. 1E) in BCG-infected mice. Infection of WT mice with *M. bovis* BCG induced a substantially delayed, significant upregulation of Mincle on the cell surface of both AM and newly recruited alveolar exudate macrophages by days 14–21 postinfection (Fig. 1F, 1G). Similarly, we observed that neutrophils immigrating into the lung at later time points after BCG challenge exhibited increased

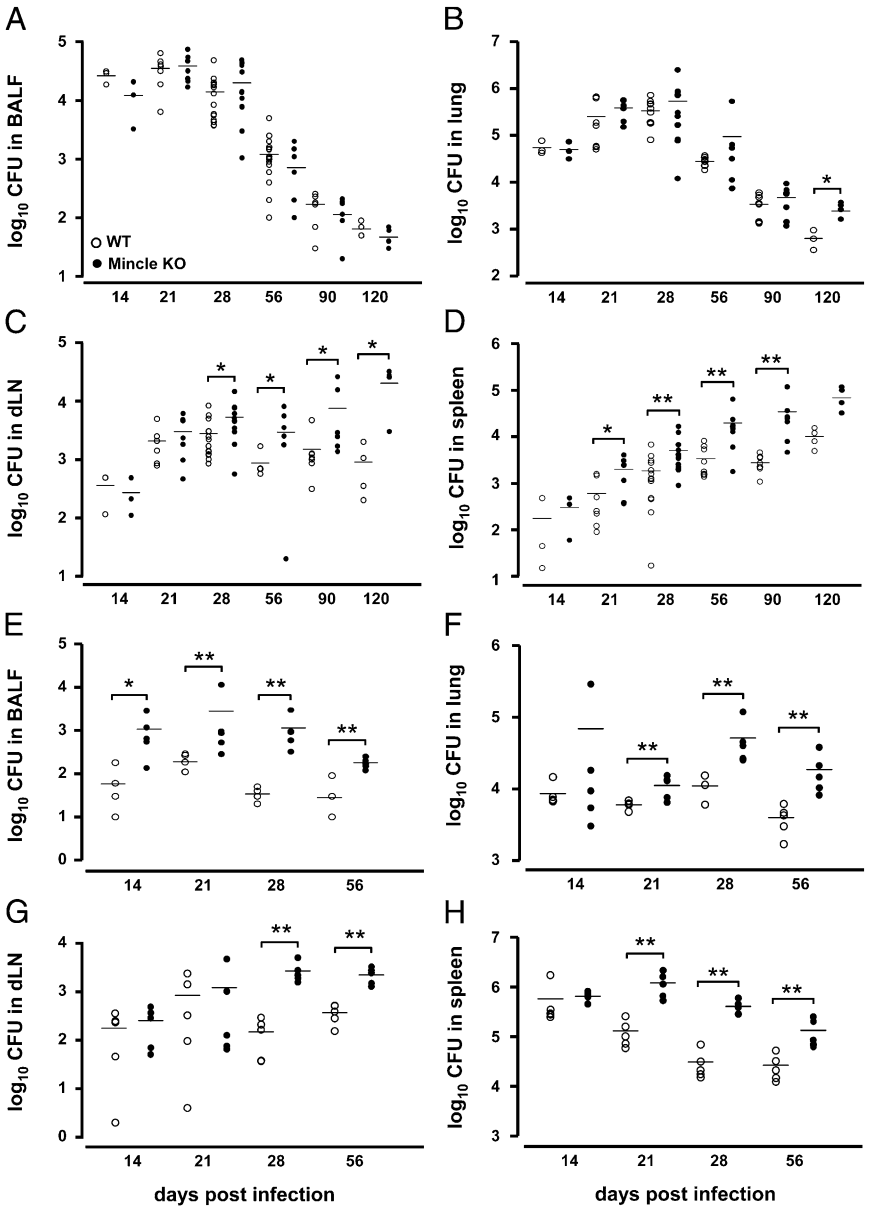

FIGURE 4. Determination of mycobacterial loads in BAL fluid, lung, lung dLN, and spleen of WT and Mincle KO mice infected with *M. bovis* BCG. WT mice and Mincle KO mice were infected with *M. bovis* BCG ($2–3 \times 10^5$ CFU/mouse) for various time intervals. At indicated time points, mycobacterial loads were determined in BAL fluid cells (**A**), lung tissue (**B**), lung dLN (**C**), and spleen (**D**) of WT mice and Mincle KO mice, as indicated. Data are shown as individual dots with $n = 7–14$ mice per time point and treatment group, except for day 14, where $n = 3$, and day 120, where $n = 4$ mice per time point and treatment group. (**E**–**H**) WT mice and Mincle KO mice ($n = 5$ mice per time point and treatment group) were infected i.v. with *M. bovis* BCG (8×10^5 CFU/mouse) and mycobacterial loads in BAL fluid cells (E), lung tissue (F), lung dLN (G), and spleen (H) were determined. Horizontal bars represent median values. $*p < 0.05$, $**p < 0.01$, relative to WT mice.

Mincle cell surface expression profiles as compared with early recruited neutrophils (Fig. 1H). At the same time, Mincle was not found to be induced on alveolar recruited lymphocytes of BCG-infected WT mice (data not shown). These data show that Mincle exhibits a delayed expression profile on AM in response to *M. bovis* BCG infection of mice.

Mincle plays an important role in proinflammatory cytokine release by primary AM stimulated with M. bovis *BCG and TDM in vitro*

Having observed that BCG was able to increase Mincle expression on primary AM in vitro, we next examined what effect a BCG challenge in the absence or presence of TDM costimulation would have on AM proinflammatory cytokine release in vitro (for experimental profile, see Fig. 2A). As shown in Fig. 2B–D, baseline proinflammatory cytokine release by vehicle-stimulated AM collected from WT and Mincle KO mice was very low. Stimulation of WT AM with TDM or BCG led to significantly increased TNF-α, MIP-2, and KC cytokine release, relative to vehicle-stimulated WT macrophages. Mincle KO macrophages demonstrated a weak cytokine release upon TDM or BCG stimulation, which was significantly lower for MIP-2 and KC (and TNF) compared with TDM-treated (or BCG-infected) WT macrophages (Fig. 2B–D). Pretreatment of WT AM with BCG for 24 h followed by restimulation of AM with TDM resulted in significantly increased release of TNF-α, MIP-2, and KC (Fig. 2B–D), relative to TDM only-treated WT macrophages, whereas BCG/TDM-treated AM of Mincle KO mice exhibited significantly reduced cytokine levels (Fig. 2B–D), relative to BCG/TDM-treated WT macrophages. However, BCG/TDM-treated Mincle KO macrophages also demonstrated a significantly increased proinflammatory cytokine release, relative to TDM only-stimulated Mincle KO macrophages. These data show that Mincle is required for maximal proinflammatory cytokine release by AM stimulated with BCG/TDM. However, in the absence of Mincle, AM are still able to respond with proinflammatory cytokines to BCG/TDM treatment, albeit at significantly lower levels as compared with WT macrophages.

Effect of Mincle on proinflammatory mediator liberation and alveolar leukocyte recruitment in mice challenged with M. bovis *BCG*

Based on the observation that AM of Mincle KO mice demonstrated a weak proinflammatory cytokine secretion after primary BCG plus secondary TDM challenge in vitro, we next examined

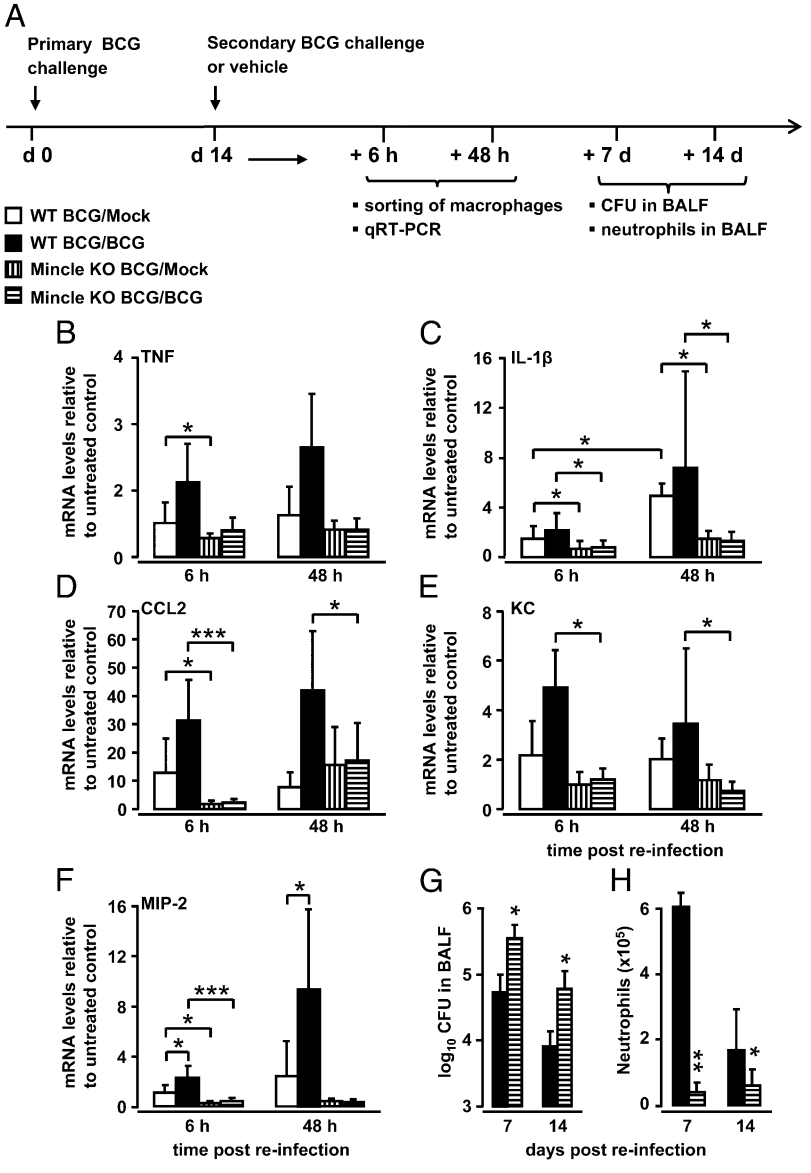

FIGURE 5. Gene expression profiles of sorted AM and antimycobacterial responses in WT and Mincle KO mice challenged with *M. bovis* BCG. WT mice and Mincle KO mice were infected intratracheally with PKH26-labeled *M. bovis* BCG ($2–3 \times 10^5$ CFU/mouse) to induce Mincle on AM (**A**). Fourteen days after infection, WT mice and Mincle KO mice were reinfected with BCG or vehicle (PBS/0.1% HSA). At 6 and 48 h after secondary infection, AM of WT or Mincle KO mice were flow-sorted and gene expression profiles of TNF (**B**), IL-1β (**C**), CCL2 (**D**), KC (**E**), and MIP-2 (**F**) were analyzed by real-time RT-PCR. (**G** and **H**) On days 7 and 14 after reinfection of WT mice and Mincle KO mice with *M. bovis* BCG, mycobacterial loads (G) and numbers of recruited neutrophils (H) were determined in BAL fluids of WT mice (filled bars) and Mincle KO mice (lined bars). Values in (B)–(F) are shown as means ± SD. Numbers of mice per experimental group were $n = 8$ mice for 6 and 48 h each of WT BCG/mock versus Mincle KO BCG/mock conditions, and $n = 9$ mice for 6 and 48 h each of WT BCG/BCG versus Mincle KO BCG/BCG conditions, compared with untreated WT mice or Mincle KO mice ($n = 3$ mice/group). In (G) and (H), values are shown as means ± SD of $n = 5$ mice per time point and treatment group. $*p < 0.05$, $**p < 0.01$, $***p < 0.001$, as indicated.

whether the absence of Mincle would also affect proinflammatory mediator liberation and subsequent alveolar leukocyte recruitment in the lungs of BCG-infected WT and Mincle KO mice. As shown in Fig. 3, significant differences in BAL fluid levels of proinflammatory cytokines TNF-α, CCL2, KC, IFN-γ, and RANTES were observed between Mincle KO mice and WT mice infected with BCG, but with variable kinetics (Fig. 3A–E). Significant differences between groups were observed for BAL fluid TNF-α levels (days 28, 56), CCL2 levels (day 28), and KC levels on day 90 postinfection (Fig. 3C). Similarly, BAL fluid levels of RANTES differed on day 21 postinfection between BCG-infected WT and Mincle KO mice, whereas no differences between groups were observed between days 28 up until day 90 postinfection (Fig. 3E). However, Mincle KO mice responded with significantly impaired recruitment of exudate macrophages, as well as neutrophils and lymphocytes to *M. bovis* BCG infection, relative to WT mice (Fig. 3F–H). No significant differences in numbers of AM between WT and Mincle KO mice were observed under these experimental conditions (data not shown).

Role of Mincle in lung protective immunity against M. bovis *BCG challenge*

In the next set of experiments, we examined the lung host defense of WT mice and Mincle KO mice against low-dose *M. bovis* BCG challenge (2–3 $\times$ 10^5 CFU/mouse). As shown in Fig. 4A–D, we found relatively similar mycobacterial loads in BAL fluids of WT versus Mincle KO mice during the first 90 d postinfection, although significantly increased CFU were observed in lung tissue of Mincle KO mice by day 120 postinfection (Fig. 4A, 4B). However, compared with WT mice, Mincle KO mice infected intratracheally with *M. bovis* BCG demonstrated significantly increased mycobacterial loads in both lung dLN and spleen as early as 21–28 d postinfection (Fig. 4C, 4D).

Dissemination of mycobacteria into extrapulmonary organs is one of the most disastrous clinical consequences of TB in humans (21). To further examine the effect of Mincle deficiency on control of mycobacterial infection in extrapulmonary organ systems, WT mice and Mincle KO mice were i.v. infected with *M. bovis* BCG at 8 $\times$ 10^5 CFU per mouse, following recently published protocols (15). As shown in Fig. 4E–H, i.v. infection of mice with BCG led to significantly increased mycobacterial loads in all examined compartments, including the bronchoalveolar space, lung tissue, lung dLN, and spleens of Mincle KO mice relative to WT mice. These data further support the conclusion that Mincle plays an important role in the control of mycobacterial infection in both pulmonary and extrapulmonary organ systems.

Mincle regulates proinflammatory macrophage activation during lung mycobacterial infections

Based on the observed similar mycobacterial loads in the lungs of WT and Mincle KO mice during the first 90 d intratracheal infection with BCG, and further given that AM and exudate macrophages of WT mice demonstrated a delayed upregulation of Mincle on their cell surface by days 14–21 after BCG challenge, we hypothesized that primary BCG challenge of AM (to fully induce Mincle on their cell surface) would increase the antimycobacterial response of these cells to secondary BCG infection (see schematic illustration in Fig. 5A), similar to the observed BCG priming effect noted in TDM-stimulated AM in vitro (see Fig. 2). As shown in Fig. 5B–F, real-time RT-PCR analysis of flow-sorted AM of WT mice subjected to primary and secondary BCG challenge revealed increased cytokine gene expression profiles of TNF, IL-1β, CCL2, KC, and MIP-2 at 6 h and particularly at 48 h after secondary BCG challenge (for primer details, see Table 1). However, results reached statistical significance only for MIP-2 at both 6 and 48 h after secondary BCG challenge, when comparing BCG/mock- versus BCG/BCG-infected AM of WT mice. However, flow-sorted AM of Mincle KO mice demonstrated far less upregulated proinflammatory gene expression after both primary and secondary infection with *M. bovis* BCG (Fig. 5B–F). Importantly, as opposed to the lack of differences in mycobacterial loads between BCG-challenged WT versus Mincle KO mice (see Fig. 4A), Mincle KO mice reinfected on day 14 with BCG demonstrated significantly increased mycobacterial loads in their lungs at both 7 and 14 d after secondary BCG challenge, relative to WT mice (i.e., at days 21 and 28 after primary BCG challenge) (compare Fig. 4A with Fig. 5G). At the same time, Mincle KO mice showed a nearly completely attenuated alveolar neutrophil recruitment at both days 7 and 14 after secondary BCG challenge (Fig. 5H).

Table I. Primer sequences used for real-time RT-PCR

Primer	Sequence (5′→3′)	Accession No.
β-actin	CCACAGCTGAGAGGGAAATC TCTCCAGGGAGGAAGAGGAT	NM_007393.3
TNF	CATCTTCTCAAAATTCGAGTGACAA TGGGAGTAGACAAGGTACAACCC	M13049
IL-1β	TGGTGTGTGACGTTCCCATT CAGCACGAGGCTTTTTTGTTG	NM_008361.3
CCL2	CTTCTGGGCCTGCTGTTCA CCAGCCTACTCATTGGGATCA	NM_011333.3
KC	CAAGAACATCCAGAGCTTGAAGGT GTGGCTATGACTTCGGTTTGG	NM_008176
MIP-2	ATCCAGAGCTTGAGTGTGACGC AAGGCAAACTTTTTGACCGCC	NM_009140

Discussion

In the present study, we examined the role of Mincle in lung protective immunity against *M. bovis* BCG. We provide evidence that 1) Mincle is induced with delayed kinetics on the cell surface of AM and newly immigrating lung exudate macrophages of BCG-infected WT mice; 2) Mincle plays a vital role in alveolar cytokine and chemokine release and the concomitantly developing alveolar leukocyte immigration in response to BCG infection; 3) compared to WT mice, Mincle KO mice respond with increased mycobacterial loads to BCG challenge particularly in lung dLN and spleen, but not in BAL fluids and lung tissue (however, Mincle KO mice are much more susceptible to i.v. infection with BCG when compared with WT mice); and 4) Mincle-deficient AM respond with significantly reduced proinflammatory cytokine gene expression to primary and secondary *M. bovis* BCG infection in vivo, relative to AM from BCG infected WT mice. These data support the concept that Mincle is an important pattern recognition receptor regulating proinflammatory responses of AM upon mycobacterial challenge.

Previous studies by Matsumoto et al. (6) and Flornes et al. (7) identified Mincle as a novel C-type lectin particularly expressed on macrophages and dendritic cells as well as neutrophils in response to several inflammatory stimuli, including LPS, TNF-α, IL-6, and IFN-γ. Use of Mincle KO mice revealed that Mincle plays an important role in *C. albicans*-induced macrophage TNF responses, whereas Mincle was not essential for phagocytosis of *C. albicans* by macrophages. However, Mincle KO mice were more susceptible to systemic candidiasis (12). More recently, Mincle was identified as an activating receptor coupled to an ITAM-containing adaptor FcRγ, and it was shown to sense SAP130 protein released by necrotic cells, as well as a receptor for the pathogenic fungus, *Malassezia* (8, 11). Reports by Ishikawa et al. (10) and Schoenen et al. (9) demonstrating a role for Mincle in

TDM-induced macrophage activation were the first studies providing evidence for a role of Mincle as pattern recognition receptor for mycobacterial recognition by professional phagocytes. Along this line, Lee et al. (14) were the first to show a role for Mincle in TDM-induced neutrophil activation and proinflammatory mediator release in mice, all of which was attenuated in Mincle KO mice.

However, until now, there were no reports examining the role of Mincle in lung protective immunity against intact mycobacterial pathogens over time. The present study adds to recent reports by establishing an important role for Mincle in the regulation of AM proinflammatory responses to *M. bovis* BCG infection in mice. Particularly, we observed that both proinflammatory cytokine/chemokine release as well as leukocyte subset recruitment during an observation period of 90 d were strongly, yet not completely, inhibited in *M. bovis* BCG-infected Mincle KO mice, suggesting that chemokine and leukocytic responses to BCG challenge may follow, at least in part, Mincle-independent signaling pathways, possibly involving signaling via TLR2 (14). Notably, Mincle-deficient bone marrow-derived macrophages were recently shown to respond with a partially impaired MIP-2 but not TNF-α release to stimulation with heat-killed *M. tuberculosis* (10), and Mincle KO mice challenged with *M. tuberculosis* demonstrated at least partially increased proinflammatory cytokines. Such observations in *M. tuberculosis*-challenged Mincle KO mice likely reflect the indirect consequence of higher bacterial burden along with the greater virulence of *M. tuberculosis* as compared with the currently employed *M. bovis* BCG, thereby causing additional inflammatory responses in mice (14).

We observed similar mycobacterial loads in the lungs of WT mice and Mincle KO mice after a single intratracheal BCG challenge. In this regard, several aspects need to be considered. First, AM of BCG-infected WT mice exhibited a strongly delayed Mincle expression kinetics, thus most likely rendering WT mice phenotypically and functionally similar to KO mice, at least during the acute phase of mycobacterial infection, where no significant upregulation of Mincle was observed on AM of BCG- relative to mock-infected WT mice. Such delayed Mincle expression by lung sentinel cells may be explained by the fact that Mincle is a ligand-inducible gene, and ligand-induced autoamplification of Mincle, together with the observation that Mincle-mediated responses are slow compared with TLR responses (22) may, at least in part, explain the observed delayed Mincle expression kinetic on AM in vivo. Second, although Mincle KO mice responded with reduced alveolar leukocyte recruitment to infection with BCG, the observed residual Mincle-independent leukocytic responses most probably may have supported control of mycobacterial replication within the lungs of mutant mice. When considering differences in CFU in secondary lymphoid organs between groups, we hypothesize that as opposed to the lung, which was challenged with a bolus application of BCG, mycobacterial loads in lung dLN and spleen were slowly increasing over time, which may have caused an improved priming of WT sentinel cells to respond with increased Mincle upregulation upon BCG challenge, thereby increasing Mincle-dependent immediate early immune responses in these organs. Further experiments are needed to identify Mincle-expressing leukocyte subsets in spleens of mice as well as their Mincle-dependent activation kinetics upon systemic *M. bovis* BCG infection.

The observed delayed expression of Mincle on AM subsequent to primary BCG infection increased their responsiveness to a secondary mycobacterial challenge in mice, as judged by significantly decreased mycobacterial loads along with higher alveolar neutrophil counts observed in the lungs of WT mice compared with Mincle KO mice after a primary and secondary BCG challenge. These data identify C-type lectin Mincle as a "delayed-type" regulator of lung phagocyte activation during mycobacterial infections in mice, taking both Mincle-expressing macrophages and neutrophils into account. Moreover, these data indicate that pattern recognition receptors other than Mincle cannot fully compensate for the lack of Mincle-dependent macrophage activation observed in the present study in response to BCG, further supporting the importance of Mincle in the regulation of AM activation during lung mycobacterial infections. The present report further adds to the study by Lee and colleagues (14) employing *M. tuberculosis* infections in mice, although in that report, only limited time points postinfection were examined.

In summary, in this study we show that Mincle is an important pattern recognition receptor regulating alveolar macrophage activation during lung mycobacterial infections in mice. Its delayed expression kinetics on resident and recruited phagocyte subsets suggests that Mincle is primarily involved in the late rather than immediate early antimycobacterial response in mice.

Acknowledgments

We acknowledge the Consortium for Functional Glycomics for providing Mincle KO mice.

Disclosures

The authors have no financial conflicts of interest.

References

1. World Health Organiation. 2011. *Global Tuberculosis Control 2011.* World Health Organization, Geneva, Switzerland.
2. Russell, D. G. 2011. *Mycobacterium tuberculosis* and the intimate discourse of a chronic infection. *Immunol. Rev.* 240: 252–268.
3. Gideon, H. P., and J. L. Flynn. 2011. Latent tuberculosis: what the host "sees"? *Immunol. Res.* 50: 202–212.
4. Marakalala, M. J., L. M. Graham, and G. D. Brown. 2010. The role of Syk/CARD9-coupled C-type lectin receptors in immunity to *Mycobacterium tuberculosis* infections. *Clin. Dev. Immunol.* 2010: 567571.
5. Russell, D. G., B. C. VanderVen, W. Lee, R. B. Abramovitch, M. J. Kim, S. Homolka, S. Niemann, and K. H. Rohde. 2010. *Mycobacterium tuberculosis* wears what it eats. *Cell Host Microbe* 8: 68–76.
6. Matsumoto, M., T. Tanaka, T. Kaisho, H. Sanjo, N. G. Copeland, D. J. Gilbert, N. A. Jenkins, and S. Akira. 1999. A novel LPS-inducible C-type lectin is a transcriptional target of NF-IL6 in macrophages. *J. Immunol.* 163: 5039–5048.
7. Flornes, L. M., Y. T. Bryceson, A. Spurkland, J. C. Lorentzen, E. Dissen, and S. Fossum. 2004. Identification of lectin-like receptors expressed by antigen presenting cells and neutrophils and their mapping to a novel gene complex. *Immunogenetics* 56: 506–517.
8. Yamasaki, S., E. Ishikawa, M. Sakuma, H. Hara, K. Ogata, and T. Saito. 2008. Mincle is an ITAM-coupled activating receptor that senses damaged cells. *Nat. Immunol.* 9: 1179–1188.
9. Schoenen, H., B. Bodendorfer, K. Hitchens, S. Manzanero, K. Werninghaus, F. Nimmerjahn, E. M. Agger, S. Stenger, P. Andersen, J. Ruland, et al. 2010. Cutting edge: Mincle is essential for recognition and adjuvanticity of the mycobacterial cord factor and its synthetic analog trehalose-dibehenate. *J. Immunol.* 184: 2756–2760.
10. Ishikawa, E., T. Ishikawa, Y. S. Morita, K. Toyonaga, H. Yamada, O. Takeuchi, T. Kinoshita, S. Akira, Y. Yoshikai, and S. Yamasaki. 2009. Direct recognition of the mycobacterial glycolipid, trehalose dimycolate, by C-type lectin Mincle. *J. Exp. Med.* 206: 2879–2888.
11. Yamasaki, S., M. Matsumoto, O. Takeuchi, T. Matsuzawa, E. Ishikawa, M. Sakuma, H. Tateno, J. Uno, J. Hirabayashi, Y. Mikami, et al. 2009. C-type lectin Mincle is an activating receptor for pathogenic fungus, Malassezia. *Proc. Natl. Acad. Sci. USA* 106: 1897–1902.
12. Wells, C. A., J. A. Salvage-Jones, X. Li, K. Hitchens, S. Butcher, R. Z. Murray, A. G. Beckhouse, Y. L. Lo, S. Manzanero, C. Cobbold, et al. 2008. The macrophage-inducible C-type lectin, Mincle, is an essential component of the innate immune response to *Candida albicans*. *J. Immunol.* 180: 7404–7413.
13. Kingeter, L. M., and X. Lin. 2012. C-type lectin receptor-induced NF-κB activation in innate immune and inflammatory responses. *Cell. Mol. Immunol.* 9: 105–112.
14. Lee, W. B., J. S. Kang, J. J. Yan, M. S. Lee, B. Y. Jeon, S. N. Cho, and Y. J. Kim. 2012. Neutrophils promote mycobacterial trehalose dimycolate-induced lung inflammation via the Mincle pathway. *PLoS Pathog.* 8: e1002614.
15. Srivastava, M., A. Meinders, K. Steinwede, R. Maus, N. Lucke, F. Bühling, S. Ehlers, T. Welte, and U. A. Maus. 2007. Mediator responses of alveolar

macrophages and kinetics of mononuclear phagocyte subset recruitment during acute primary and secondary mycobacterial infections in the lungs of mice. *Cell. Microbiol.* 9: 738–752.
16. Mailaender, C., N. Reiling, H. Engelhardt, S. Bossmann, S. Ehlers, and M. Niederweis. 2004. The MspA porin promotes growth and increases antibiotic susceptibility of both *Mycobacterium* bovis BCG and *Mycobacterium tuberculosis. Microbiology* 150: 853–864.
17. Steinwede, K., R. Maus, J. Bohling, S. Voedisch, A. Braun, M. Ochs, A. Schmiedl, F. Länger, F. Gauthier, J. Roes, et al. 2012. Cathepsin G and neutrophil elastase contribute to lung-protective immunity against mycobacterial infections in mice. *J. Immunol.* 188: 4476–4487.
18. Steinwede, K., O. Tempelhof, K. Bolte, R. Maus, J. Bohling, B. Ueberberg, F. Länger, J. W. Christman, J. C. Paton, K. Ask, et al. 2011. Local delivery of GM-CSF protects mice from lethal pneumococcal pneumonia. *J. Immunol.* 187: 5346–5356.
19. Schreiber, O., K. Steinwede, N. Ding, M. Srivastava, R. Maus, F. Länger, J. Prokein, S. Ehlers, T. Welte, M. D. Gunn, and U. A. Maus. 2008. Mice that overexpress CC chemokine ligand 2 in their lungs show increased protective immunity to infection with *Mycobacterium bovis* bacille Calmette-Guérin. *J. Infect. Dis.* 198: 1044–1054.
20. Livak, K. J., and T. D. Schmittgen. 2001. Analysis of relative gene expression data using real-time quantitative PCR and the $2(-\Delta\Delta C_T)$ method. *Methods* 25: 402–408.
21. Dorhoi, A., S. T. Reece, and S. H. Kaufmann. 2011. For better or for worse: the immune response against *Mycobacterium tuberculosis* balances pathology and protection. *Immunol. Rev.* 240: 235–251.
22. Werninghaus, K., A. Babiak, O. Gross, C. Hölscher, H. Dietrich, E. M. Agger, J. Mages, A. Mocsai, H. Schoenen, K. Finger, et al. 2009. Adjuvanticity of a synthetic cord factor analogue for subunit *Mycobacterium tuberculosis* vaccination requires FcRγ-Syk-Card9-dependent innate immune activation. *J. Exp. Med.* 206: 89–97.